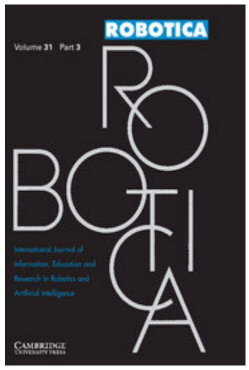

Air jets imaging tactile sensing device for automation applications

R. Benhadj and B. Dawson

Robotica / Volume 13 / Issue 05 / September 1995, pp 521 - 529
DOI: 10.1017/S0263574700018361, Published online: 09 March 2009

Robotica (1995) volume 13, pp 521–529. © 1995 Cambridge University Press

Air jets imaging tactile sensing device for automation applications

R. Benhadj and B. Dawson

On-Line Surveillance, Monitoring and Diagnostics Unit (OSMAD), School of Mechanical and Production Engineering, Kingston University, Roehampton Vale, Friars Avenue, London SW15 3DW (UK)

(Received in Final Form: October 4, 1994)

SUMMARY
This paper details the design principles of operation of a pneumatic proximity-to-tactile sensing device for part handling and recognition in a flexible manufacturing environment. The sensing device utilises a densely packed line array of piezoresistive pressure sensors, providing continuous variable outputs. The sensing plane of the device incorporates a corresponding line array of air jets which develop an air cushion when striking a target of interest. The back pressure levels from these air jets form the basis for the task of target detection and recognition.

KEYWORDS: Tactile sensing; Automation; Pressure sensors; Air jets imaging.

1. INTRODUCTION
In developing a tactile sensing system, an overall structure is usually adhered to which takes the following form.

- A discretely distributed array of sensing sites is planned;
- a corresponding number of signal conditioning circuits are devised for the purpose of data acquisition;
- a medium or a membrane is used to transmit the effect of the desired stimulus to the sensing sites.

The sensing array consists of sensing elements that are transducers which ideally respond to a form of stimulus such as pressure,[1–3] light,[4,5] heat[6,7] or displacement.[8] The signal conditioning is used to relate the output record of the transducer (usually voltage or current) to the magnitude of the stimulus source. A medium or membrane is usually used to transmit the effect of the external stimulus to the transducer, whilst in many cases protecting the sensing elements from environmental conditions. For instance, soft membranes such as rubber are used to prevent direct contact of a metallic object with a piezoresistive *IC* pressure sensor in order to avoid damage to the sensor and short circuiting it. However, rubber allows direct transmission of pressure stimulus to the *IC* pressure sensor.

In designing tactile sensing arrays, a number of important factors must be considered. The most important consideration is to ensure that an adequate sensing resolution for a given application is planned for. The sensing resolution is further subdivided to spatial resolution (i.e. positioning) of sensing elements in the array (on the surface of the sensing plane), and the measurement sensitivity of the sensing elements at each locality. Tactile sensing is a relatively new technology, and has been mainly applied within the field of robotics. In this field, tactile sensors have been developed and used to emulate the human sense of touch. Therefore, the sensing resolution is often planned to closely approximate human mechanoreceptive capabilities. Complex configurations of tactile sensing, such as those of humans, are beyond the scope of the current state of the art. Most tactile sensing devices are devised to respond to the changes relating to a specific parameter of interest such as pressure or displacment. The sensing resolution along the sensing plane of approximately 1 mm is found to be close to human touch reception.[9] In terms of pressure stimulus, the most sensitive part of the skin is on the index finger, having a detection resolution of 6 μm indentation or 6.8–10 grammes per centimetre square for a comfortable touch.[10]

Other considerations include the choice of the sensing element and the substrate or matrix that contains the sensing elements. With the transducer (i.e. sensing element), one important consideration is to ensure that a continuously variable output is achieved. This refers to the sensor's capability to respond to changes in the value of the applied stimulus in a continuous fashion. The measurement characteristics of the sensing elements should ideally be linear, hysteresis free and have a fast response time.[11,12] In reality, however, all sensing elements exhibit non-linear characteristics somewhere in their working range. An important consideration is therefore the extent of the operating range for which a linear response to an external stimulus can be expected. The same consideration is also true of the effect of hysteresis. For instance, with piezoelectric strain gauges,[13] the sensor response is quite non-linear and can be affected by hysteresis when the device is supplied with a constant voltage. A constant current supply can be used with this device in order to ensure a more linear output response.

Other factors that might affect the performance of tactile sensors are fatigue of the membrane or substrate, drift in conductivity or saturation, noise and environmental conditions. Miniaturisation of sensing elements has two main advantages. Firstly, it enhances the sensing resolution as denser arrays of these elements can be constructed. Secondly, with smaller devices problems due to non-linearity diminish. Miniature single crystal silicon sensing devices can now be machined, giving a robust micromechanical structure.

In this paper, a novel design of a high resolution pneumatic proximity-to-tactile sensing device is developed based on a line array of back pressure air jets which monitor any change in the pressure of an air cushion. The air cushion pressure is generated by an air flow which strikes a target, and the air flow leaves an air chamber through an air nozzle. Each back pressure air jet is designed so that it is completely isolated from the air flow in the air chamber in order to avoid any interference between the air flow in the air chamber and the back pressure air jet. The design of the high resolution proximity-to-tactile sensing device was developed via a number of iterative designs to meet the demands of a flexible, robust and cheap to manufacture sensing device.

2. PRINCIPLE OF DESIGN AND OPERATION

In this paper the design principles of operation of a hard compliant tactile sensing device is presented. The reason for opting for a hard compliant device is that it enables repetitive use without having to make contact between the sensing plane and objects of interest, thereby eliminating problems such as wear and damage that might be caused to the sensing plane. In choosing a hard compliant device, an active medium must be used to transmit the effect of the external stimulus to the sensing element. A fluid or light are the obvious choices since they are cheap, wear resistant and easy to obtain. Dry air in particular is available in most industrial plants and laboratories. It has no corrosive or contaminating action as other fluids may have, and requires very little control as is usually required when light is used as a transmitting medium. Therefore, it was specified that the design would be centred around the use of air as a transmitting medium.

With air, two different approaches to measurements can be adopted. Firstly, pressure can be utilised as a parameter which responds to the changes caused by the external stimulus. Secondly, flow rate or flow velocity may be used. The former was selected as it would correspond more directly to pressure receptance in cutaneous tactile sensing. In order to ensure sufficient sensing resolution, air flow should be concentrated as jets and the pressure would normally be monitored from individual corresponding sensing elements. The configuration chosen was to measure the back pressure to an air jet striking a target. Each jet was then considered as a source of excitation (stimulus) that is monitored by a corresponding back pressure jet that leads to a sensing element. In this way one may control the source of stimulation (air jet pressure), monitor the feedback (back pressure jet) and ascertain information about the target which affects the feedback pressure. An array of such supply air jets and corresponding back pressure feedback jets can provide quantitative information about the profile of target surfaces.

2.1 Air flow in the tactile sensing block

To assist in the design of the sensing device, an understanding of the theoretical behaviour of air flows in the sensing device is helpful and is developed via the three stages shown in Figure 1 and represented as Flow A, Flow B and Flow C. Flow A is the air flow leaving the air chamber of the sensing block through a nozzle. The air flow is developed between the air chamber and the sensing plane. Flow B is the air flow between the sensing plane and the target, and Flow C is the air flow through the back pressure air jet.

A large volume air chamber is constructed in order to maintain a constant pressure supply. The length of the back pressure air jet is kept to a minimum in order to reduce the pressure losses along the air jet length and also to increase the volumetric flow accordingly. This also ensures a sufficient pressure gradient between the jet's inlet and the atmosphere to sustain a high flow rate through the air chamber and the back pressure air jet.

The velocity distribution of the air which flows steadily parallel to the axis in the annular space between two coaxial cylinders of radii R and r_1 (i.e. Flow A) as shown in Figure 2, is given by the following equation (1).

Where μ is the air viscosity.

$$V_x = \frac{dp}{4\mu\, dx}(r^2 + a_1 \ln r + a_2) \tag{1}$$

From the velocity distribution $V_x(r)$ as shown in Figure 2, the two constant of integration A and B are determined from the following boundary condition.

$$V_x = 0 \quad \text{at} \quad r = R \quad \text{and} \quad r = r_1$$

From these boundary conditions, the constants of integration a_1 and a_2 are determined as follows:

$$a_1 = -\frac{\left(\left(\frac{R}{r_1}\right)^2 - 1\right)r_1^2}{\ln\left(\frac{R}{r_1}\right)^2}; \quad a_2 = \frac{\left(\left(\frac{R}{r_1}\right)^2 - 1\right)r_1^2}{\ln\left(\frac{R}{r_1}\right)^2}(\ln r_1 - r_1^2) \tag{2 \& 3}$$

Therefore by substituting the two constant of integrating equations (2) and (3) in equation (1), the air jet velocity becomes:

$$V_x = -\frac{dp}{4}\mu\, dx\left[(r_1^2 - R^2) + \frac{\left(\left(\frac{R}{r_1} - 1\right)\right)r^2}{\ln\left(\frac{R}{r_1}\right)}\ln\left(\frac{r}{r_1}\right)\right] \tag{4}$$

The rate of volumetric flow is derived by double integrating the velocity:

$$Q_x = \iint V_x r\, dr\, d\theta \tag{5}$$

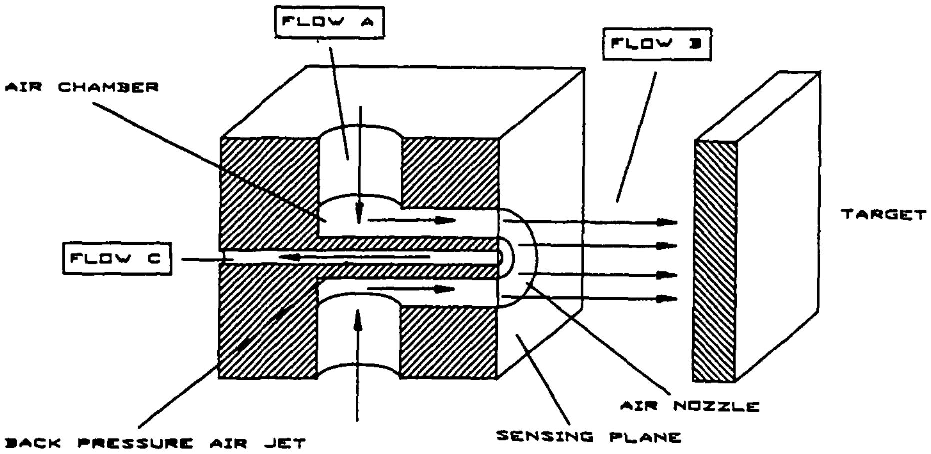

Fig. 1. Air flow in the tactile sensor configuration.

and hence the pressure drop along the air jet is given by the following equation:

$$dp = -\frac{8\mu Q_x\, dx}{\Pi r_1^4}\left[\frac{\ln\left(\frac{R}{r_1}\right)}{\left(\ln\left(\frac{R}{r_1}\right)\left(\left(\frac{R}{r_1}\right)^4 - 1\right) - \left(\left(\frac{R}{r_1}\right)^2 - 1\right)\right)}\right] \tag{6}$$

From equations (1) and (2), the pressure drop (dp) can be calculated and therefore the pressure (P_2) of the air flow leaving the air chamber through the nozzle can be evaluated. The flow rate through the air chamber and the pressure entering the air chamber (P_1) are set by a flowmeter and pressure regulator respectively.

When an air flow strikes a solid surface (i.e. a target of interest), it does not rebound from the surface as a rubber ball would rebound. Instead, some of the air flow escapes on all sides of the target and an air cushion is formed in between the sensing plane and the target as illustrated in Figure 3(i), 3(ii) and 3(iii). The air flow leaves the air chamber with a velocity and pressure as defined by equations (1) and (2). This creates a pressure at the surface of the target as an air cushion and this is assumed to be as follows:

$P_{\text{cushion}} = $ (*Pressure leaving air chamber* − *Pressure loss*)

The pressure loss between the sensing plane and the target surface is related to the gap size (dx). Therefore, as the gap (dx) between the sensing plane (or the end of the air chamber) and the target surface reduces, the pressure loss decreases accordingly. It can therefore be inferred that as the gap (dx) reduces, the air cushion pressure tends to equal the pressure leaving the air chamber and therefore the pressure at the entrance of the back pressure air jet. Another important factor is the force of the air flow that strikes the target surface. This force should not exceed the force necessary to hold the target in equilibrium. the force normal to the target surface is determined as follows:

$$F_x = \rho V_x Q_x \tag{7}$$

where: ρ is the density of air.

The air flow through a straight pipe of circular cross-section with axial symmetry (in this case the back

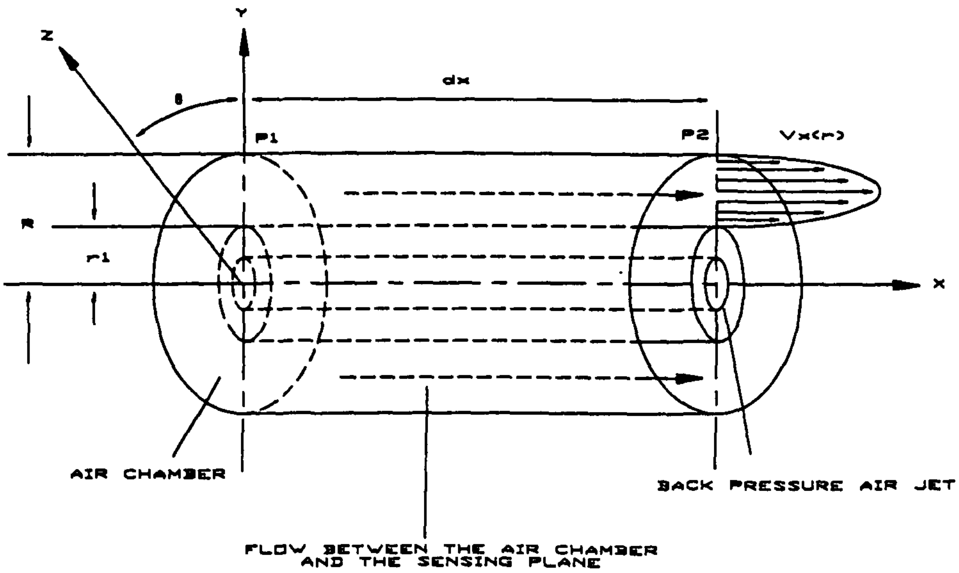

Fig. 2. The air flow between the air chamber and the air jet nozzle.

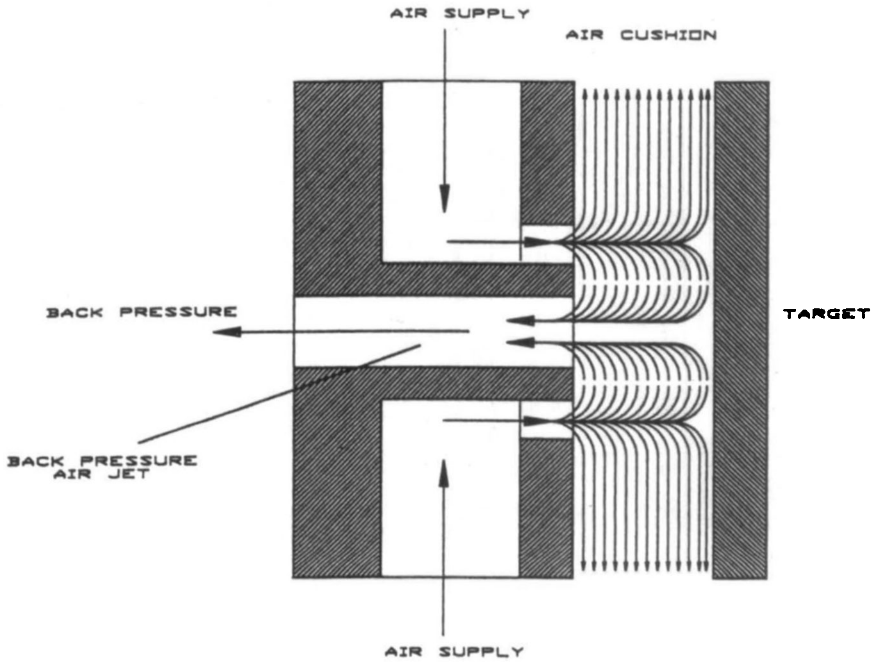

Fig. 3(i). Flow distribution over a flat target.

pressure air jet) is similar to the preceding case as governed by *Poiseuille's* law applicable to blood flow in narrow vessels. Figure 4 illustrates the flow through a back pressure air jet where the volumetric flow rate Q_x through the entire cross-section is given by the following equation:[14]

$$Q_x = \pi R^2 V_{av} \tag{8}$$

The average velocity in Hagen-Poiseuille flow,[14] can be obtained as follows:

$$V_{av} = \frac{1}{\pi R^2} \iint V_x r \, dr \, d\theta \tag{9}$$

From equations (4) and (5), (dp) is the pressure change through the back pressure air jet $(P_2 - P_1)$. P_2 is the pressure at the entrance in the air jet and is approximately equal to the pressure of the air cushion. P_1 is the exit air pressure through the back pressure air jet which is monitored by the *IC* pressure sensor. If it is assumed that the back pressure air jet length (dx) is very short so that the pressure drop in the back pressure air jet tends to zero, then the input air jet pressure (or air cushion pressure) can be assumed to be equal to the exit pressure and therefore to the *IC* pressure sensor. From this assumption, the flow rate Q_x through the back

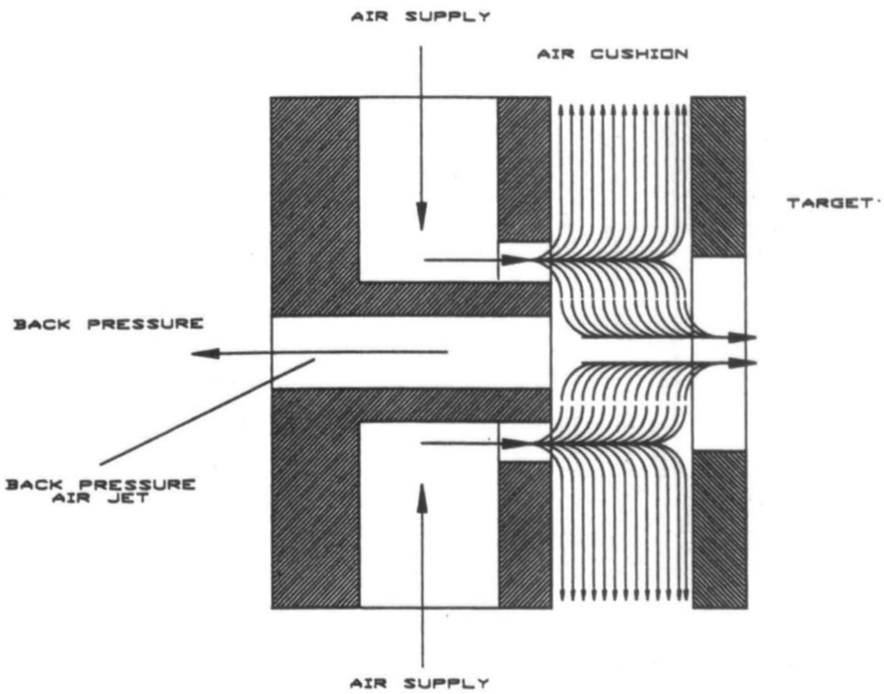

Fig. 3(ii).. Flow distribution over a hemisphere.

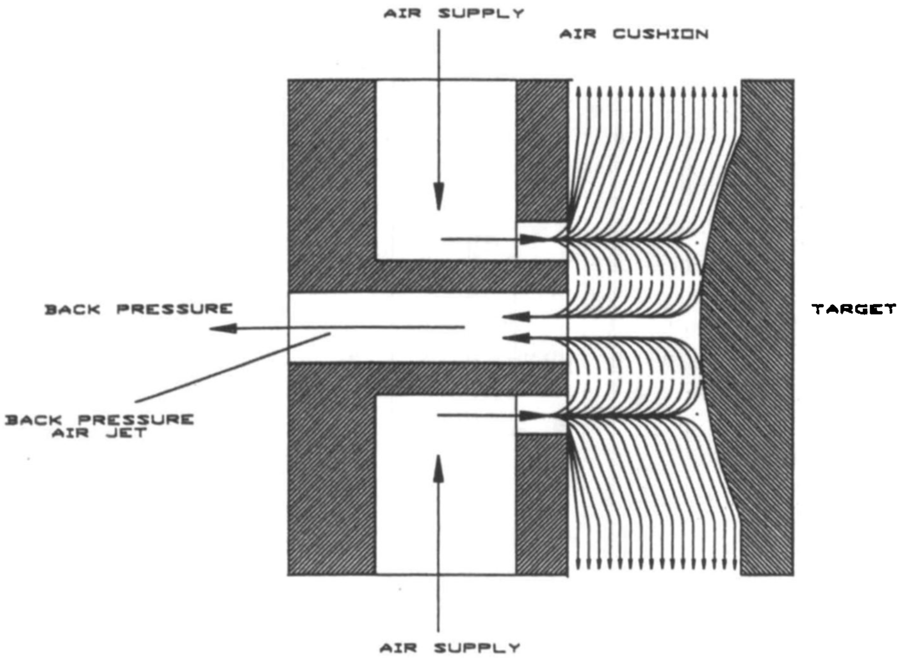

Fig. 3(iii). Flow distribution over a hemisphere.

pressure air jet can be evaluated from equations (4) and (5). Knowing the input flow rate through the air chamber, the flow rate and pressure loss between the sensing plane of the sensor block and the target can be approximated.

Any decrease in the air jet length (dx) will result in a decrease of the pressure loss in the air jet as mentioned above. Thus the shorter the air jet the less pressure drop is obtained in the air jet. This is one important design consideration, while another consideration is the diameter of the back pressure air jet. In designing the tactile sensor, the diameter should be as small as possible to enable a number of air jets to be compacted in a small area in order to achieve a high spatial resolution device. Equations (4) and (5) suggest that with a larger back pressure air jet diameter a lower pressure drop is achieved.

The theory outlined above proves useful in understanding the effect of parameters such as the dimensions of the air chamber, the nozzle diameter and the length and diameter of the back pressure air jet. These parameters are very important in the tactile sensor design. The derived equations are also helpful in determining the amount of air supply one needs in order to meet the design requirement. A low pressure supply will limit the tactile sensor sensing sensitivity. Although a higher pressure supply increases the tactile sensor sensitivity, higher pressure can destroy the *IC* pressure sensor element. It is therefore desirable to supply the device with an optimum pressure supply.

3. SIGNAL ACQUISITION AND PROCESSING

A simple electronic circuit is used to monitor the signal generated by the pressure sensor. A constant current of 1 mA is used to energise the bridge circuit formed by the

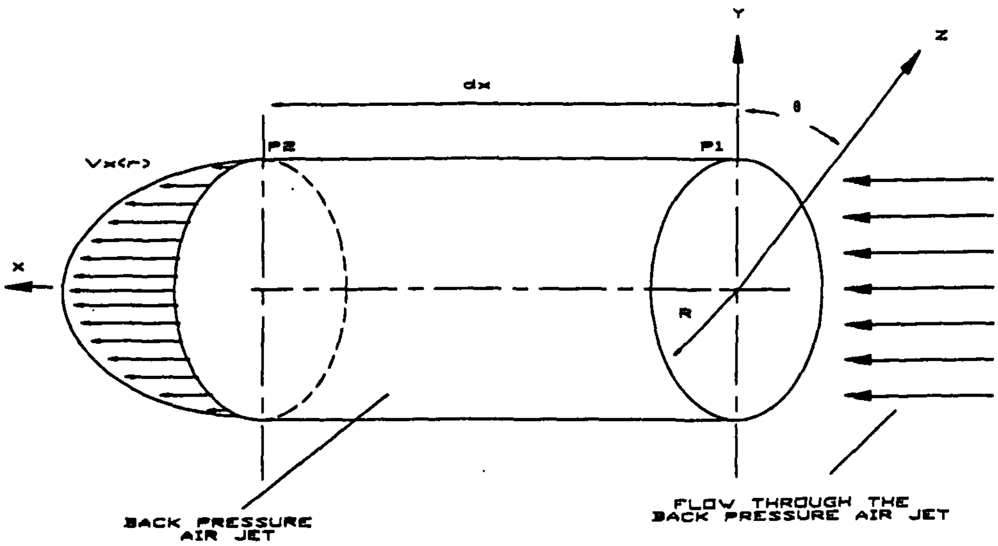

Fig. 4. Air flow through a back pressure air jet.

four piezoresistive strain gauges. A high precision potentiometer is incorporated within the bridge circuit which allows the calibration of the output signal of the span (bridge circuit output) and sets it to a zero reading at any back pressure. The analogue signal generated by the bridge circuit (the sensor span) is then amplified by a high input impedance differential *JFET* type operational amplifier with an output voltage gain of 17.8. A combination of a diode and a zener diode are used at the output to prevent the signal from being dropped to a value under 0 volt (or precisely negative signals) or to signals exceeding 5 volts as the signals are subsequently fed to a digital circuit (A/D analogue to digital converter). The amplified analogue signal goes through an analogue to digital converter before the signal is processed.

3.1 Sensing element

The sensing element employed is a piezoresistive *IC* pressure sensor which uses a mechanical spring element in the form of a diaphragm. The back pressures are directed along the hollow tubes, applied to the spring elements, and converted into mechanical strains which in turn provide continuous voltage outputs. The diaphragm is usually fabricated by employing a special anisotropic etching technique. This allows a number of diaphragms to be produced on a thin silicon wafer. A pyrex constraint plate is bonded to the silicon diaphragm plate in order to isolate the sensing element from the package stress. The silicon diaphragm is subjected to the differential pressure ($P_1 - P_2$), where P_2 is the pressure at which both plates were sealed together and corrected for operating temperature. To measure the stress in the N-type silicon diaphragm, four *P*-type resistors (strain gauges) are employed. These strain gauges are obtained through a selective diffusion of boron into the silicon diaphragm, and the bonding between the strain gauges and the diaphragm is achieved through the atomic structure of silicon. This type of bonding eliminates the effect of creep, which is the major source of instability in metaliic or bonded types of strain gauge sensors.

Two of the strain gauges are located in an area of compression, while the other two are in an area of tension. Electrically they are interconnected into a fully active Wheatstone bridge configuration to maximise the output signal. This bridge provides an analogue output signal which is proportional to the input pressure. The full-scale span for this type of integrated sensor is 100 mV. The particular type of IC pressure sensor used in this sensing device has the following features:

- good solid state stability;
- low noise susceptibility;
- temperature compensation over the range of 0–50°C;
- high resolution graded output in the range of 0–15 Psi (gauge pressure) with an accuracy of 0.1%;
- small weight, approximately 3 grammes.

Variable resistors in the conditioning circuit board should compensate or the *IC* pressure sensor by enabling it to work in the range of 0 to 50°C with a ±1% error in the output signals (loaded and unloaded span). This temperature compensation is described.[15]

4. SENSING BLOCK

The sensing block is described in detail in [15] and is assembled to the signal conditionning circuit box via two rigid brackets on each side of the block and should be kept normal to the sensing plane of the sensing block. The piezoresistive pressure sensors are connected to the sides holes of the sensing block via flexible tubes. Flexible tubing is also used for the air supplied to the chamber. Each piezoresistive pressure sensor is connected to an individual variable resistor of an electrical circuit and the output signals are transmitted to the computer interface through a 20 way ribbon plug as shown in Plates 1 and 2.

The prototype design of the proximity-to-tactile sensing block utilises the air jets in such a fashion that the tactile sensor has an acceptable spatial resolution (air jets spacing) and also a good sensitivity response. The other major consideration is the ease and cost of producing the tactile sensing device. Furthermore, the position of the air jets must be selected in such a way so as to ensure that the air supply jets do not impinge on the sides of the column and cause turbulent conditions to occur. The spatial resolution of this tactile device depends directly on the size of the back pressure air jets, as smaller the diameter of the back pressure air jets, the better the spatial resolution. The ideal tactile sensor as described by Professor Harmon[9] exhibits a spatial resolution of 1 mm and this emulates the human touch sensing. In this configuration, the size and the means of machining the air jets columns do not allow us to perform the ideal spatial resolution. In order to achieve a reasonnable spatial resolution without affecting the sensitivity of the device a method of scanning the same line of the target twice by sifting the sensing device by half of the its spatial resolution.[15,16]

The measurement resolution (or sensitivity) of the device was obtained by mounting the sensing block on a vertical computer controlled milling machining centre. A flat slab of material (a test piece) was held underneath the spindle on the machine bed and in a pneumatically operated jaw. The supply pressure and the volumetric flow rate were kept constant and the sensor block was advanced in the direction of the test piece (or target), reducing the gap in increments of 10 μm. When the gap was less than 1 mm, a discernable change in the values of the *IC* pressure sensor output was observed for any increment of motion. The measurement resolution (i.e. sensitivity) was found to be 1 mV/μm. With the *CNC* machine movement sensitivity of 10 μm, it is impossible to fulfil the capabilities of the sensor. However, if a precise automated platform is used, the device would be capable of discerning object features down to a micron. Therefore, the tactile sensing device can be employed for detection of anomalies such as cracks and burrs on object surfaces but not to ascertain surface textures.

The pneumatic proximity-to-tactile sensor monitors

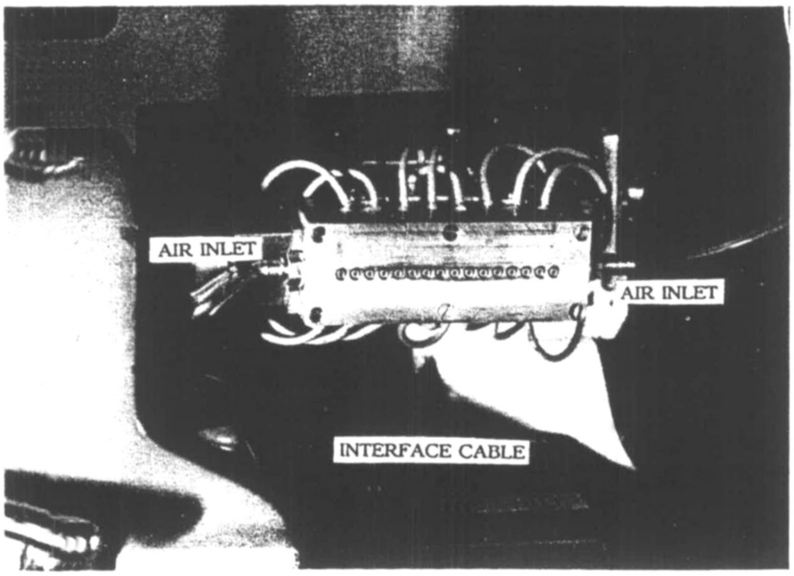

Plate 1. Imaging tactile sensing device front view.

object profiles by measuring the gap between the sensing plane and the object surface. The sensor output is an array of analogue signals from *IC* pressure sensors in terms of mV. In using the tactile sensor, it is necessary to calibrate it in order to obtain a relationship between mV output and the gap depth. The calibration curve varies with the supply pressure and the volumetric flow rate. For a constant condition (i.e. constant supply pressure and volumetric flow rate), the calibration characteristic curves of each individual sensing element of the proximity-to-tactile sensor device at different gap sizes between the sensing plane and the object to be sensed are fully described in reference.[15] It should be noted that each *IC* pressure sensor has its own calibration curve. Once a line array of mV values are converted to gap depths using the appropriate calibration curves, the profile of the object surface facing the sensing plane would be known.

5. TACTILE IMAGE RECONSTRUCTION

Plate 3 shows the recognition system setup which consists of a very accurate X-Y-Z platform with a $\pm 10\,\mu m$ accuracy for each axis. The positions of the three axes are monitored by a digital displays. The sensing device is firmely fixed to Z axis and free to move in the X-Y-Z axis. The sensing device is fed with air from a regulated pressure supply line. Each pressure sensor circuit of the sensing device is supplied by ±15 Volts from a power supply. The analogue signal from the pressure sensor are processed and amplified before being converted to digital signal by an A/D convertor. The digital signal from each channel of the convertor is interfaced an I/O interface board. The signals are then accessed by a data acquisition and processing algorithm.[15,17]

If we consider the idea of an image from the simplest point of view we could regard an image as a two-dimensional function, where the value of the

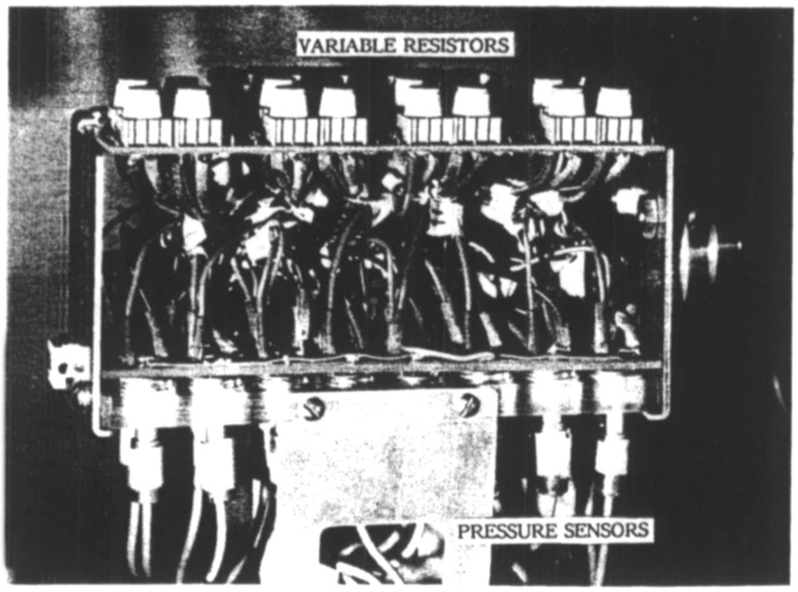

Plate 2. Imaging tactile sensing device side view.

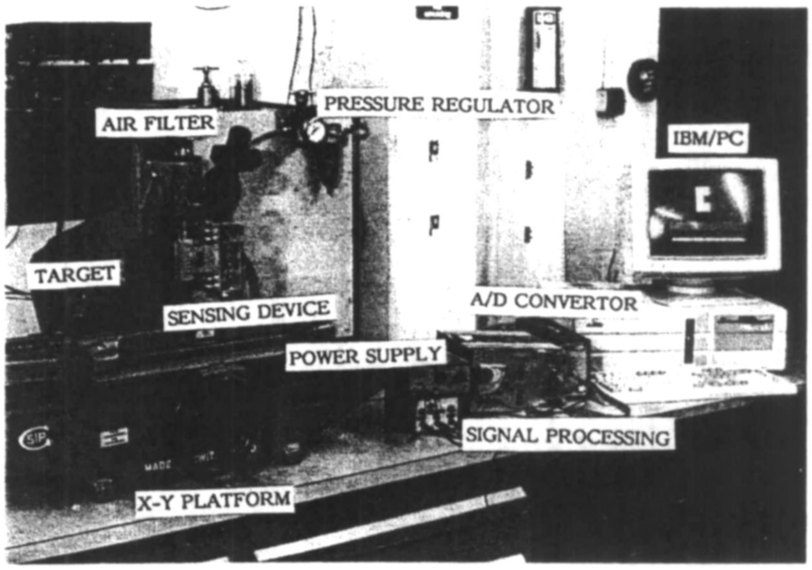

Plate 3. Image reconstruction set up.

function $f(x, y)$ at spatial cordinates (x, y) in the X–Y plane defines a measure of the back pressure resulting from the proximity-to-tactile sensor. For our purposes, where ease of computer-based processing is a primary requirement, we shall be concerned with digital images, where we accept a suitable approximation of the function $f(x, y)$ in return for convenience in representation and subsequent processing. A digital image is an image which has been approximated in two ways, corresponding to spatial and amplitude digitization.

Sometimes referred to as image sampling, this involves representing the national original continuous image function as an array of specific samples at discrete points within the two-dimensional frame of reference, as illustrated in above. In general, the spatially digitized image consists of (x, y) equally distributed samples, where each discrete point in the array is identified as a picture element or taxel in this case.

Each taxel in the array has to encode the local image value. An image intensity (back pressure reading) level is designated a grey level and the full range of intensity levels available in a particular image is referred to as the grey level. In this case, we are concentrating on binarized images, where the amplitude digitization occurs when the grey level consists of just two possible levels (0 and 1), as the resulting image consists of an array of points each of which is either black or white. It is clear that binary images are simple to generate, store and manipulate, since each taxel is associated with a single bit of information, provided that we retain enough information for subsequent processing requirements, there are many

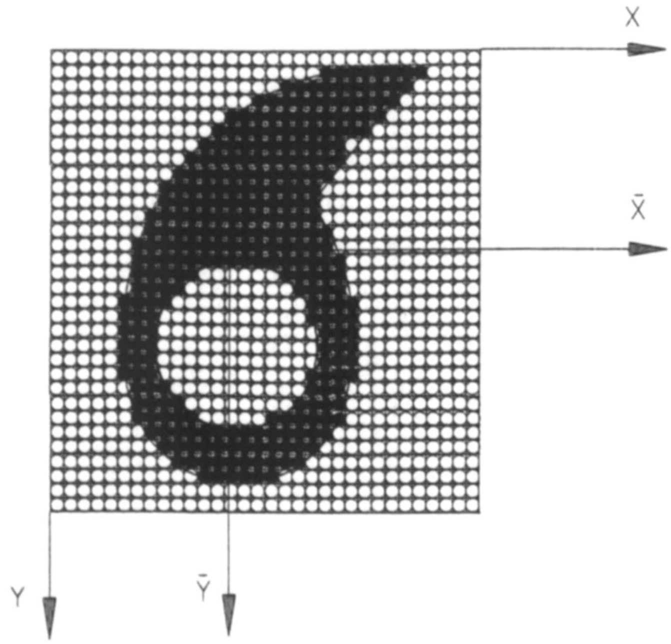

Fig. 5(i). Computer binary image reconstruction of a cam at 0° orientation.

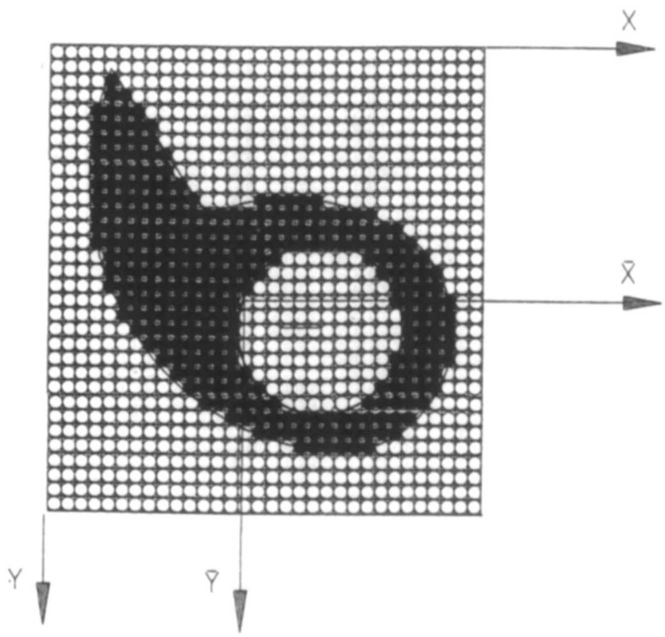

Fig. 5(ii). Computer binary image reconstruction of a cam at 45° anti-clockwise orientation.

advantages in working with binary images where possible in practical situations. Figure 5(i) and 5(ii) represent a computer binary reconstruction of a cam at two different orientations which comprises an array of 32 × 32 circular sensing sites, 1.5 mm diameter and 3 mm center to center spacing, and it is approximated to human finger resolution.

6. CONCLUSION

The tactile sensing device presented in this paper can acquire object related information that corresponds closely to the human sense of touch. The information obtained is rather limited in diversity when compared with the human tactile capability. However, within its narrow band of cutaneous emulation the analysis performed provides quantitative information that is not usually acquired by human touch reception. This sensing device provides information in a narrower bandwidth than that of a vision system. It acquires lower resolution global information than vision. This makes tactile sensing more useful for feature extraction (i.e. holes) and object recognition using predicates than for global image processing. Therefore, it is concluded that the device should acquire high resolution from predefined locations within an object view. In this mode tactile data information acquisition and processing can resolve in object recognition in a faster cycle than with visual analysis.

The other features of this tactile sensing device is firstly less affected by environmental conditions such as lighting, smoke, or haze which affect visual processing and other tactile sensing. It does also not suffer from problems associated with most tactile sensors such as wear, fatigue, hysteresis and drift in conductivity because of its data acquisition from a "near-tactile" mode. The devised tactile sensor can, however, suffer from noise and turbulent flow conditions. Because of its low resolution, the problem of noise can be alleviated by software compensation more readily than in the case of visual analysis. Air is used as a transmitting medium between the effect of the external stimulus to the sensing element, this medium is cheap, easy to control and more available when compared to other transmitting media such as a soft membrane, Xenon light, laser etc.

Examples of applications of such a device are:

- Objects indentification and orientation assessment[17–19]
- Gripping force monitoring
- Object slip detection.

References

1. P. Dario and D. De. Rossi, "Tactile Sensor and the Gripping Challenge" *IEEE Spect* 46–52 (August, 1985).
2. M.H. Raibert and J.E. Tanner, "A VLSI Tactile Array Sensor" *Proceedings of the 12th Int. Symp. Industrial Robots and the 6th Int. Conf. Industrial Robot Technology* Paris (1982) pp. 417–425.
3. R. Benhadj, H. Rahnajet and M. Safa, "High Resolution Pneumatic Proximity Tactile Sensing Device" *Int. J. AMT* **2**(3), 59–72 (August, 1987).
4. K. Tanie, K. Komoriya, M. Kaneko, A. Fujikawa and S. Tachi, "A High Resolution Tactile Sensor" *Proc. 4th Int. Conf. Robot Vision and Sensory Controls,* London (October, 1984) pp. 251–260.
5. J.L. Shneiter and T.B. Sheridan, "An Optical Tactile Sensor for Manipulators" *Robotics and Computer-Integrated Manufacturing* **1**(1), 65–71 (1984).
6. P. Dario, C. Domenici, R. Bardelli, D. De Rossi and P.C. Pinotti, "Piezoelectric Polymers: New Sensor Materials for Robotic Applications" *Proc. 13th Int. Symp. Industrial Robots* (1983) pp. 14–34.
7. R.A. Russell, "A Thermal Sensor Array to Provide Tactile Feedback for Robots" *Int. J. of Robotics Research* **4**(3), 35–39 (1985).
8. N. Sato, W.B. Heginbotham and A. Pugh, "A Method for Three Dimensional Part Identification by Tactile Transducer", *Proc. 7th Int. Symp. Industrial Robots* (1987) pp. 123–129.
9. L.D. Harmon, "Automated Tactile Sensing" *Int. J. Robotics Research* **1**(2), 3–32 (1982).
10. Y. Zotterman (Ed.), *Sensory Functions of the Skin in Primates*: (Pergamon Press, Oxford, 1976).
11. L. Harmon, "Touch-Sensing Technology" *Proc. Robots of the 4th Int. Conf.* (October, 80) pp. 375–390.
12. W.J. Dixon, M.B. Brown, L. Engelman, J.W. Frame, M.A. Hill, R.I. Jenrich and J.D. Roporek (Eds.), *BMDP Statistical Software* (University of California, Berkeley, California, 1983).
13. K.E. Pennywitt, "Robotic Tactile Sensing" *Byte Magazine* 177–200 (January, 1986).
14. S.W. Ynan, *Foundations of Fluid Mechanics,* SI Unit (Ed.) (Prentice-Hall Int., London, 1970).
15. R. Benhadj, *PhD Thesis* (Kingston University, UK, July, 1992).
16. R. Benhadj, B. Dawson and M. Safa, "Imaging Pneumatic Proximity-to-Tactile Sensing Device" *Sensor Review* **13**(3), 23–28 (August, 1993).
17. R. Benhadj, S. Sadeque and H. Rahnejat "A Knowledge-Based system for sensor interaction for Real-Time Component Control" *Int. J. AMR* **3**(1), 77–102 (February, 1988).
18. R. Benhadj, S. Sadeque and B. Dawson, "Tactile Binary Imaging Recognition Algorithm Using Geometrical Moment Invariants" *Sensor Review* **13**(4), 13–22 (November, 1933).
19. R. Benhadj, S. Sadeque, B. Dawson and M. Safa, "Towards Unmanned Manufacture: Applications of an Expert System" *CODEM 89 Int. Conf., Birmingham Poly.* (September, 1989) pp. 206–209.